Fretting fatigue failure of polyester resin and its glass fibre mat composites

K. FRIEDRICH
Polymer and Composites Group, Technical University Hamburg-Harburg, 2100 Hamburg 90, West Germany

When relative movement can arise between mating parts and one is subjected to cyclic stresses, then the fatigue life can be very much reduced. Such a phenomenon is referred to as fretting fatigue. In this paper, results of fretting fatigue experiments obtained with unsaturated polyester and its glass fibre mat composites are reported. In addition, some fracture and wear properties of the materials are discussed.

1. Introduction

Relative cyclic motion of two surfaces in intimate contact constitutes the condition for a wear process known as fretting. This wear process often results in a significant reduction in fatigue resistance, as known for a large number of metallic alloys [1–3]. The fretting fatigue occurs when repeated loading on a structure or part causes a sliding movement at material interfaces in the design. This movement, in turn, must induce, at or near points of contact between the faces, fatigue stresses of sufficient intensity to cause cracking [4]. There are numerous engineering situations where these requirements may be encountered. The most common ones are flanges and bolted joints [5]. Other design details that can give fretting fatigue problems are leaf springs, collars and bushes. Fibreglass-reinforced-plastics (FRP) are frequently used for such purposes, yet little has been published on the performance of these materials under fretting fatigue conditions.

The present paper, therefore, represents one of the first studies, in which a polymer composite material is investigated with respect to its general mechanical behaviour, its wear resistance, and with respect to the effect of a fretting wear component on its fatigue life.

2. Experimental techniques

2.1. Materials

Unsaturated polyester resin containing a high amount of $CaCO_3$-particles ($\sim 50\%$) was chosen as matrix material (UP). In addition, studies were carried out with two reinforced versions of the UP-matrix, nominally a 27 wt % glass fibre mat (GF) and a 37 wt % GF-UP composite, respectively. The materials were delivered from Grillo Werke, Voerde, West Germany, as ~ 5 mm thick plates ($500 \times 500\,\mathrm{mm}^2$). The reinforcing glass fibre mats consisted of continuous fibre bundles, being randomly arranged in their orientation to each other, but in-plane, i.e. more or less parallel to the plate surfaces. Schematically, this is represented in Fig. 1a. Corresponding micrographs taken from polished areas of the x–y (Fig. 1b) and y–z-plane (Fig. 1c) illustrate that (a) each fibre bundle consists of about 200 single fibres (fibre diameter $d = 10\,\mu$m), (b) there is no uniform distance between individual fibre bundles, (c) the $CaCO_3$-particles in the matrix have a size between 20 and 50 μm, (d) the matrix is interspersed with sporadic voids having dimensions similar to the diameter of the fibre bundles ($\approx 200\,\mu$m).

2.2. Testing procedures

2.2.1. Mechanical tests under static conditions

In order to get a feeling for the mechanical performance of the neat matrix material and its fibre-reinforced variants, tensile tests as well as fracture mechanics tests were carried out at room temperature and a crosshead speed of $0.5\,\mathrm{mm\,min^{-1}}$. In addition, the ball indentation hardness was measured according to German Standard DIN 53456, and for some special samples also the flexural strength according to DIN EN 63.

2.2.2. Wear studies

The resistance of a material against wear can be studied under different counterpart and loading conditions. In the present case, a single pass, abrasive wear situation (obtained by the use of Al_2O_3-paper of $D = 7\,\mu$m average grain size) was chosen. Further details of this method are described elsewhere [6].

2.2.3. Fretting fatigue tests

For the pure fatigue experiments, dog bone specimens having dimensions as given in Fig. 2a, were cyclically stressed in tension–tension at different stress levels (ratio of minimum to maximum load $R = 0.22$; frequency $f = 10$ Hz). An additional fretting component could be accomplished by two fretting pads which were attached to a frame fixed to the specimen grips. Normal forces on to the pads were applied through a colinear arrangement which could be mechanically compressed; the applied forces were controlled by a load cell. The magnitude of slip of the pads and the specimen surface was controlled by the location of the pad on the gauge length of the specimen (l_p) and the range of applied stresses (p). Thus cyclic elastic

0022–2461/86 $03.00 + .12

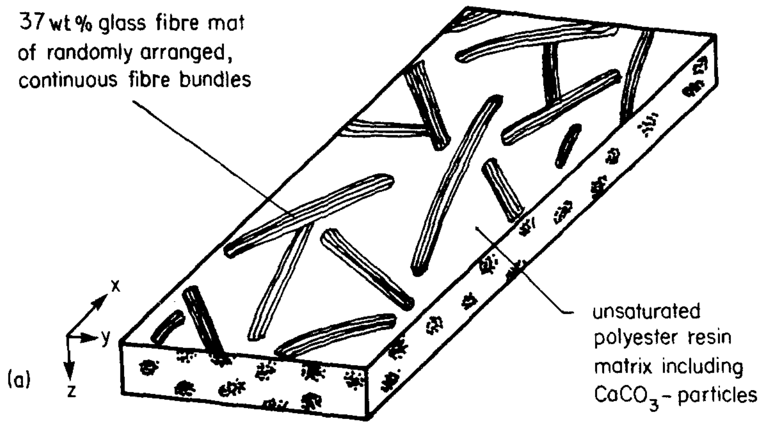

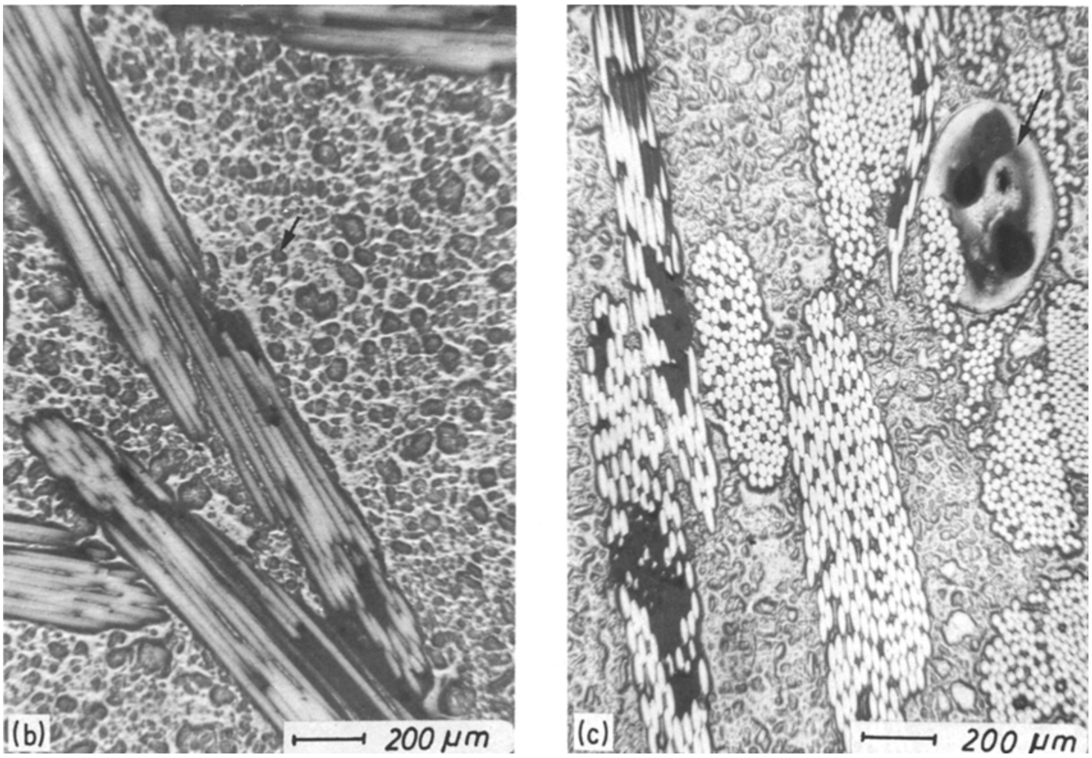

Figure 1 Microstructure of glass fibre mat-unsaturated polyester composites: (a) schematic illustration of fibre arrangement in the plates, (b) micrograph of *x–y*-plane (arrow = $CaCO_3$-particle), (c) micrograph of *y–z*-plane (arrow = void).

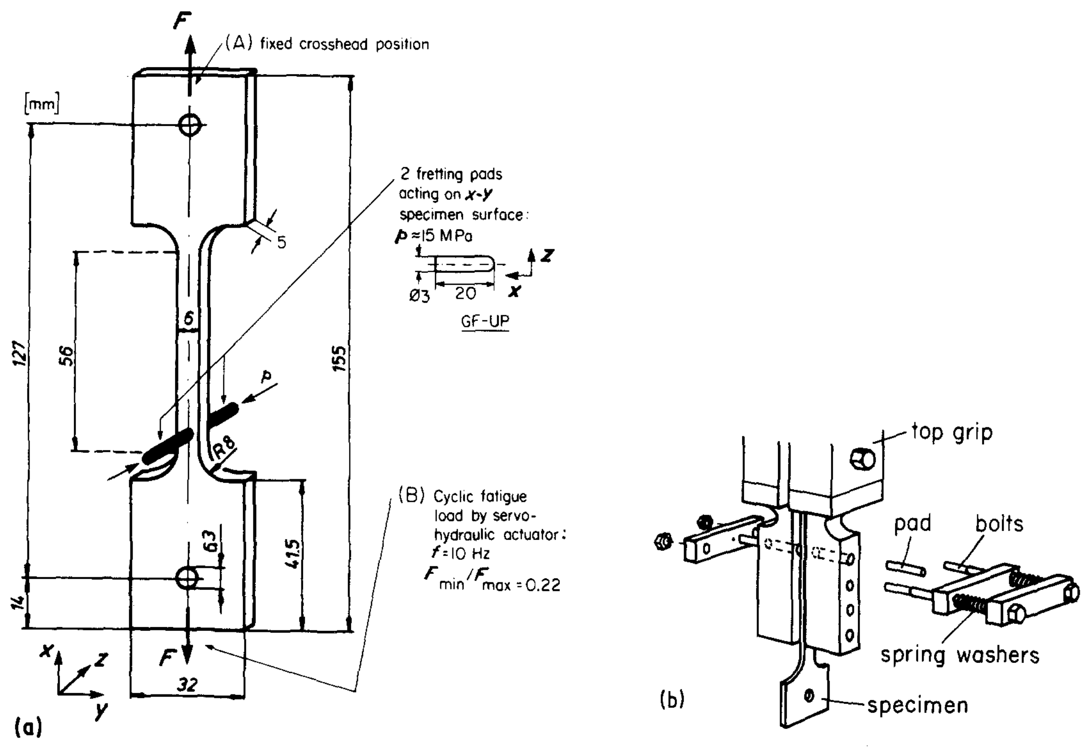

Figure 2 (a) Fretting fatigue specimen configuration and (b) schematic drawing of the fretting frame (after [3]).

TABLE I Densities and mechanical data of the polyester matrix and its composites. Opposite to the relatively high fibre weight fractions given by the manufacturer (27 and 37 wt %), lower values are obtained when using the measured densities (16 and 25 wt %). The corresponding volume fractions are then 11% and 18%, respectively (fibre density $\varrho_F = 2.55\,g\,cm^{-3}$).

Material	Density $\varrho(g\,cm^{-3})$	Direction		H (MPa)	E (GPa)	σ_B (MPa)	K_c (MPa $m^{1/2}$)
		H	σ_B, E, K_c				
UP-matrix	1.64	‖	L	205	6.9	35	1.2
		⊥	T	206	6.9	34	1.1
27 wt % GF-UP	1.74	‖	L	213	12.3	65	10.2
		⊥	T	234	13.3	71	10.0
37 wt % GF-UP	1.80	‖	L	263	13.6	82	11.1
		⊥	T	287	13.9	80	10.6

deformation in the gauge length of the specimen induced relative slip between the specimen and the "fixed" fretting pad. A schematic graph of the fretting frame is shown in Fig. 2b (after [3]). It should be mentioned that in this study l_p as well as p were held constant (see Fig. 2a). The fretting pads used here were machined out of the 37 wt % GF-UP testing material.

2.3. Failure analysis

Studies of the failure mechanisms under wear loading and under fretting fatigue conditions were performed by the use of scanning electron microscopy (SEM). Prior to the microscopic examination, specimen surfaces were coated with a thin gold layer.

3. Results and discussion

3.1. Hardness, strength and fracture toughness

The static mechanical properties measured for the three different materials of this study are summarized in Table I. As a general trend, all of the properties determined (hardness H, elastic modulus E, tensile strength σ_B, fracture toughness K_c) increase with increasing amount of fibre reinforcement. Measurements on samples taken from the plates from two directions perpendicular to each other ($L = x$; $T = y$; cf. Fig. 1a) indicate that the materials possess in-plane a quasi-isotropy of the tensile and fracture properties. The hardness, on the other hand, is different when measured on the x–y-plane (fibre bundles parallel (‖) to plate surface) compared to the y–z- or x–z-planes (dominated by ends of fibre bundles (⊥)).

Within the scatter of the fracture toughness data, there is no distinct dependence of the K_c values on the initial crack length of the compact tension specimens used (Fig. 3). Thus, the K_c values can be considered to be real material properties for the given testing conditions (crosshead speed, temperature, specimen thickness).

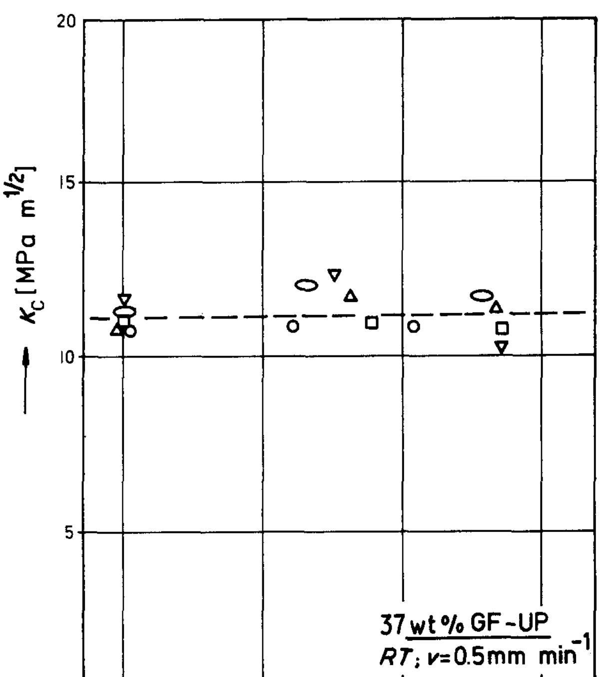

Figure 3 Fracture toughness, K_c, of 37 wt % GF-UP (L-direction) plotted against the ratio of crack length, a, to specimen width W. Different symbols refer to different specimens.

3.2. Abrasive wear performance

Fig. 4 illustrates that the specific wear rate, $\dot{w}_s$ (change in volume per load and sliding distance) is reduced the more fibres are incorporated into the polyester matrix. This improvement in wear resistance (inverse of the wear rate) is, however, different for the two different surface conditions (‖ against ⊥), as already noticed for the hardness of the material. Both, hardness and wear resistance, are typical properties which are especially dependent on the microstructural conditions at and near the surface of a material, so that this analogy is not very surprising. The coefficient of friction μ, on the other hand, did not show any

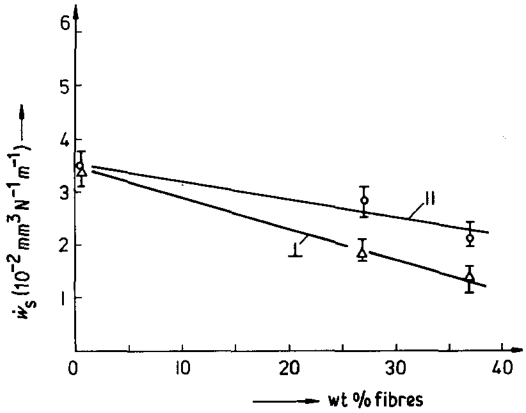

Figure 4 Specific wear rate, $\dot{w}_s$, of unreinforced and reinforced UP. The dominant fibre arrangement on the worn surfaces (‖) and (⊥) of the material are schematically illustrated in Fig. 1a. GF-UP against 7 μm Al_2O_3.

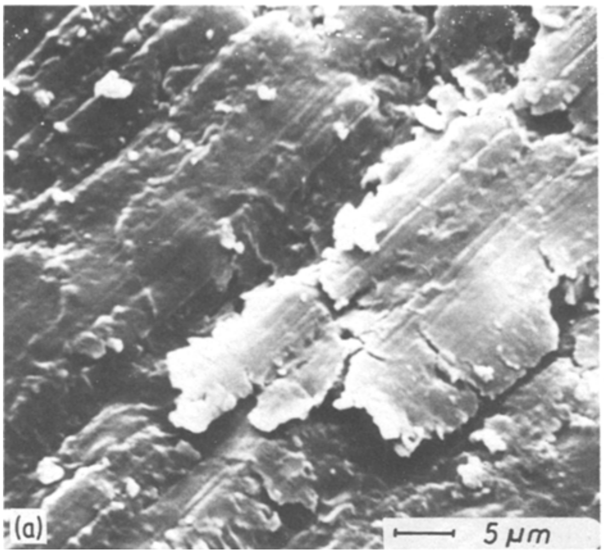

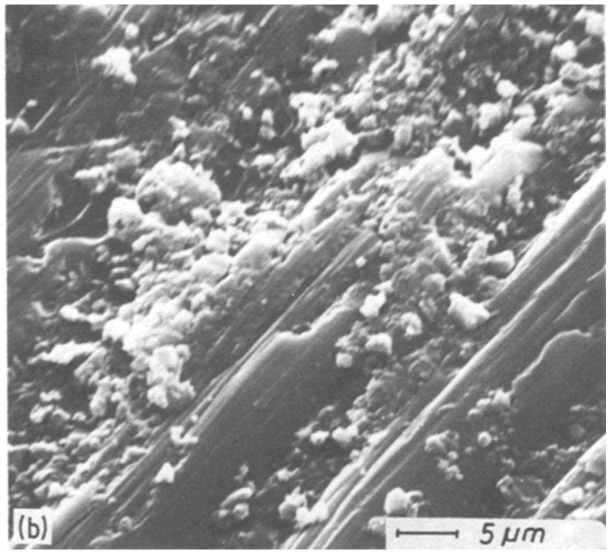

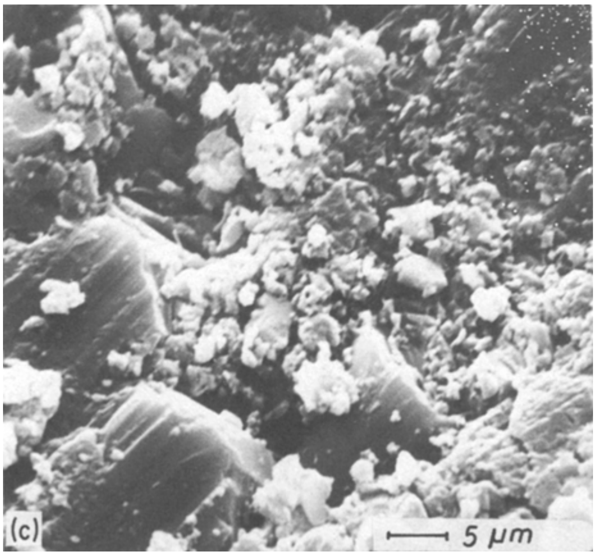

Figure 5 Scanning electron micrographs of the worn surfaces: (a) neat matrix, (b, c) fibre-reinforced samples (∥ and ⊥ surfaces).

pronounced dependence on the materials' surface morphology. For the six different conditions (two sliding directions, three materials) the frictional coefficient varied in the range 0.475 ± 0.02.

An idea about the mechanisms of material removal during wear can be achieved by the SEM analysis of the worn surfaces (Fig. 5). On the surface of the unreinforced polymer smooth matrix regions containing very fine scratches are found between deep wear furrows due to local plowing events by some of the larger counterpart asperities. In addition, cracking events underneath the surface and perpendicular to it and to the sliding direction seem to form plate-like wear debris (Fig. 5a). The latter mechanisms are suppressed by the presence of fibres, but at the cost of fibre thinning and eventually fibre cracking by the harder abrasive particles (Fig. 5b and c).

3.3. Fatigue life and fretting effects

3.3.1. Mechanical test results

Fig. 6 summarizes the results of the fatigue tests obtained without and with additional fretting load. The latter was accomplished by pressing one pad on to each side of the sample (pressure $p = 15\,\mathrm{MPa}$), at a location of the gauge length where the slip amplitude was nearly highest (cf. Fig. 2a). With respect to the fibre-reinforced samples, the surface structure subjected to the fretting condition was that of the x–y-plane seen in Fig. 1a (fibre bundles in-plane). It was expected that this condition would lead to a most pronounced effect of an additional fretting component, because this surface structure (∥) exhibited higher wear rates than the one under 90° to it (⊥). It turned out, however, that in the fibre-reinforced cases (here only presented for 37 wt % GF-UP) there was no effect of the fretting component at all. All the data fell in the same scatter band typical for regular fatigue life studies. Furthermore, most of the samples subjected to additional fretting, failed at other positions than at the fretting location (most of the time in region B of the gauge length, i.e. between the fretting pads and the fixture to the servohydraulic actuator). This was, however, quite different when tests were carried out with the unreinforced polyester resin. In relation to the fibre composites, a certain fatigue life could only be achieved at lower stress levels. In addition, a clear reduction in fatigue life due to a fretting component was noticeable (at lower stress levels by more than two orders of magnitude).

3.3.2. Failure mechanisms

The microscopic analysis of the failure mechanisms was concentrated on samples which were fatigued with an additional fretting load. Fig. 7 represents the situation of a fretting fatigued GF-UP material. The specimen finally failed at the upper edge of the fretting scar (Fig. 7a). Detailed analysis of the fretted region showed that several cracks had been initiated at this location (Fig. 7b). They are, however, highly hindered in further growth due to the presence of neighbouring, in-plane fibre bundles, crossing the crack fronts continuously (Fig. 7c). In this way, there exists a hard competition in growth rate of these cracks with those initiated at the edges and the machined sides of the sample dominated by ends of fibre bundles (Fig. 7d). The latter seem to have a greater chance to initiate and

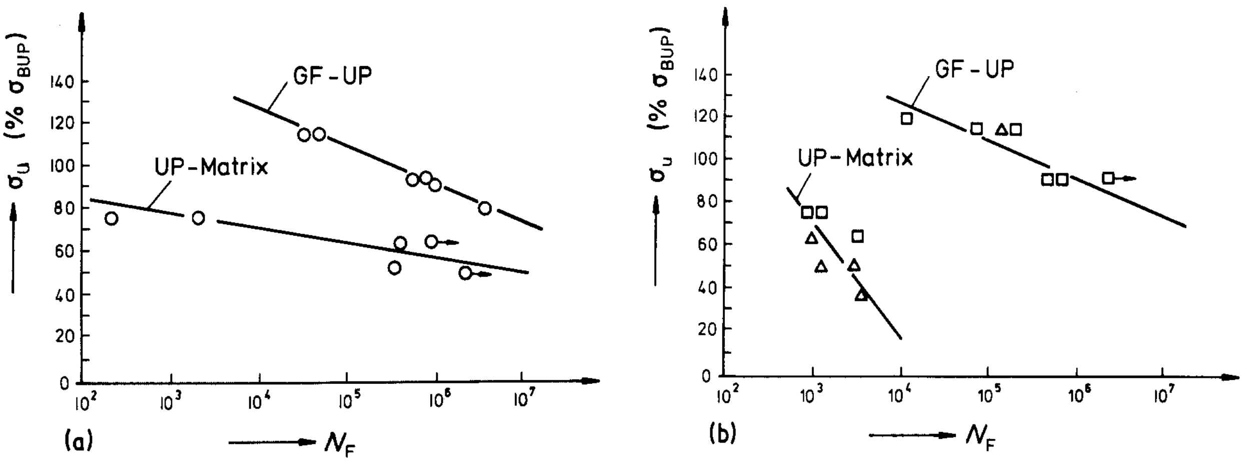

Figure 6 Upper fatigue stress (in percentage of matrix strength σ_{BUP} = 35 MPa) plotted against number of cycles to failure (N_F): (a) fatigue data without fretting (circles); (b) fretting fatigue data (squares = failure at other locations, triangles = failure at fretting scar).

propagate more easily, as a result of a more favourable fibre bundle orientation. Thus, they dominate the fatigue life of the composite even under the presence of a fretting component. Schematically, this situation is illustrated in Fig. 8. Indirect evidence for these differences in crack initiation and propagation resistance is found when measuring the flexural strength of GF-UP samples of rectangular cross-section in two different directions. The flexural strength, σ_F, is higher by a factor of more than 20% if the bending load acts in the *z*-direction relative to the *y*-direction (σ_{F_y} = 24 MPa).

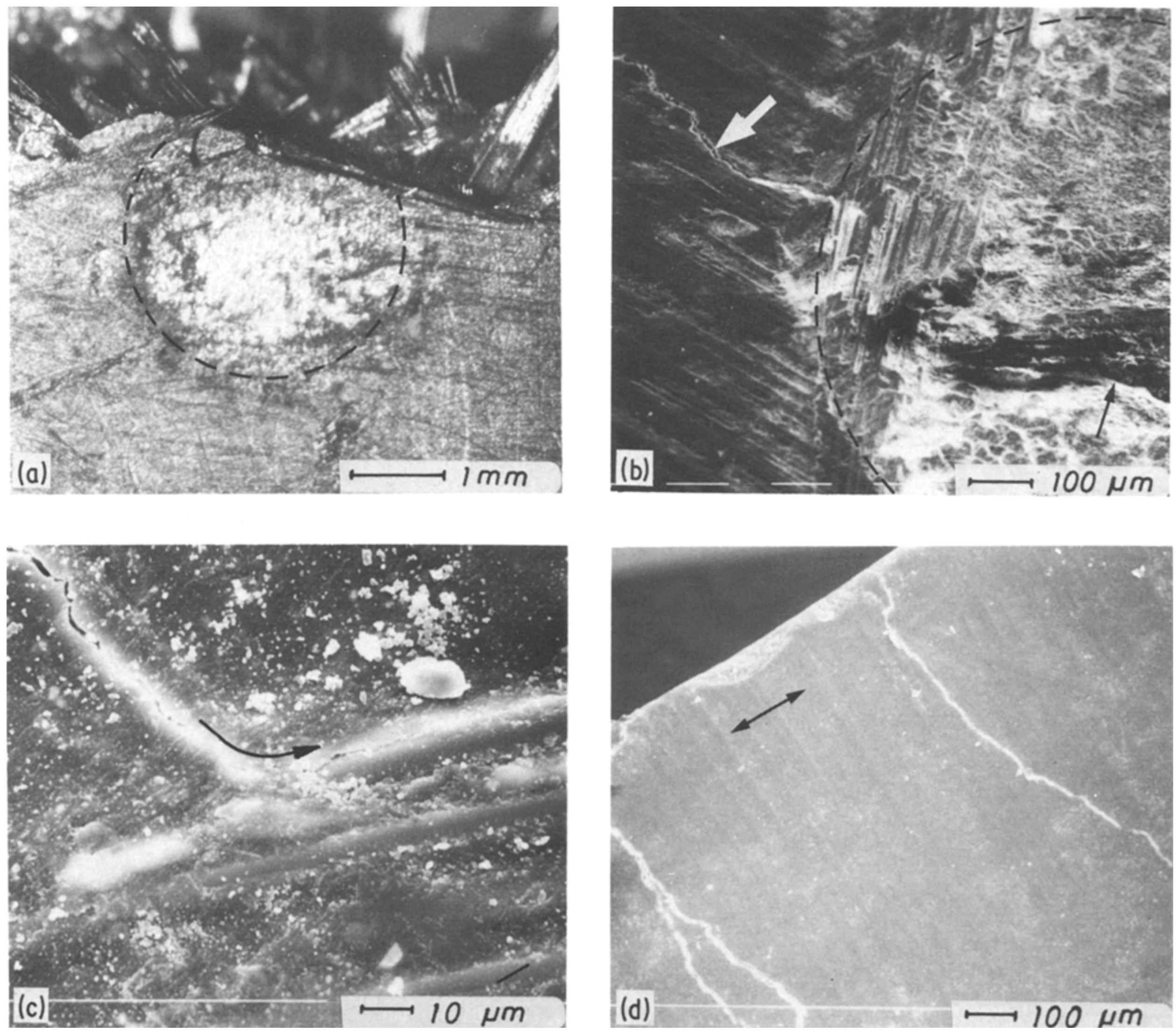

Figure 7 Scanning electron micrographs of fretting fatigued specimens of GF-UP: (a) fretting scar on the specimen surface, with final failure at this location (dashed line); (b) cracks initiated inside (black arrow) and outside (white arrow) of a fretting contact area (dashed line); (c) crack deviation and stopping at in-plane fibre bundles; (d) regular fatigue cracks initiated at the machined edge and far away from the fretted region. The double arrow indicates the direction of the fatigue load.

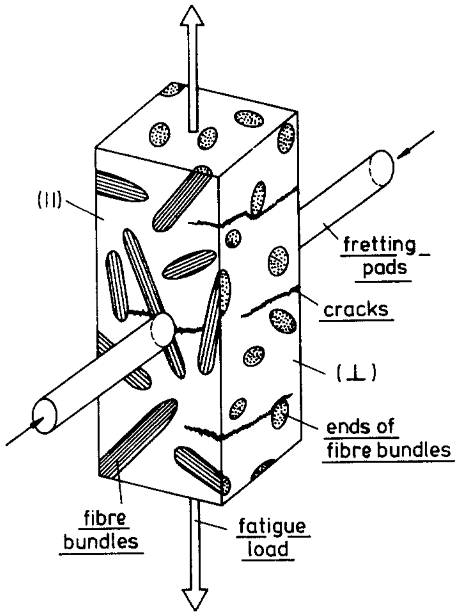

Figure 8 Schematic illustration of crack competition in fretting fatigued GF-UP-specimens.

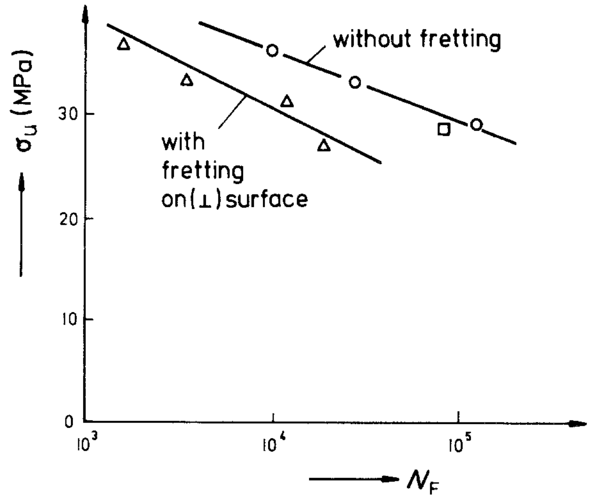

Figure 9 Effect of fibre orientation relative to the fretting pad on the fretting fatigue life of 27 wt % GF-UP-samples (for meaning of symbols see Fig. 6). $R = 0.22, f = 5$ Hz.

In other words, it must be expected, that the effect of a fretting component on the fatigue endurance of a fibre composite material is strongly dependent on the local fibre orientation in the vicinity of the fretted scar. It can be assumed that a detrimental effect will clearly occur if the fretting actions would take place at those sides of the samples which are dominated by ends of fibre bundles (x–z-plane; cf. Fig. 2a). In fact, preliminary experiments carried out with 27 wt % GF-UP and fretting on the x–z-planes of the samples showed a clear reduction in fatigue life relative to samples without fretting (Fig. 9). That means, the more favourable condition of fibre ends perpendicular to the sliding plane in case of the wear rate studies has now changed into an unfavourable situation. Fretting fatigue cracks initiated here can propagate more easily than under in-plane fibre arrangement, thus leading to pronounced reductions in fatigue life of the composites (Fig. 10).

The micrographs presented in Fig. 11, finally give an impression on the fretting fatigue failure of the neat polyester resin samples. In most of these specimens the main crack which led to final fatigue fracture was initiated somewhere at the outer region of the fretting scar (Fig. 11a). The appearance of the corresponding fracture surface clearly reflects the development of the fatigue fracture from the fretting location at the specimen surface (centre of the lower edge on Fig. 11b). Higher magnifications of the fretted region indicate a dense pattern of smaller and wider surface cracks which had formed perpendicular to the slip direction (Fig. 11c). This effect is, of course, independent of which side of the sample the fretting action takes place. Occasionally, larger voids are found on the fracture surface, which can also act as sites of fatigue crack initiation (Fig. 11d). They might be a reason for the fact that especially under low cycle fatigue conditions (higher stresses) samples with fretting failed at other positions.

4. Conclusions

The results of an experimental programme to examine mechanical properties and especially the fretting fatigue behaviour of unsaturated polyester resin and its glass fibre mat composites have been presented in this paper. The glass reinforcement improves significantly the hardness, tensile strength, fracture toughness, abrasive wear resistance, and the fatigue life of the polymer matrix. The endurance limit is, however,

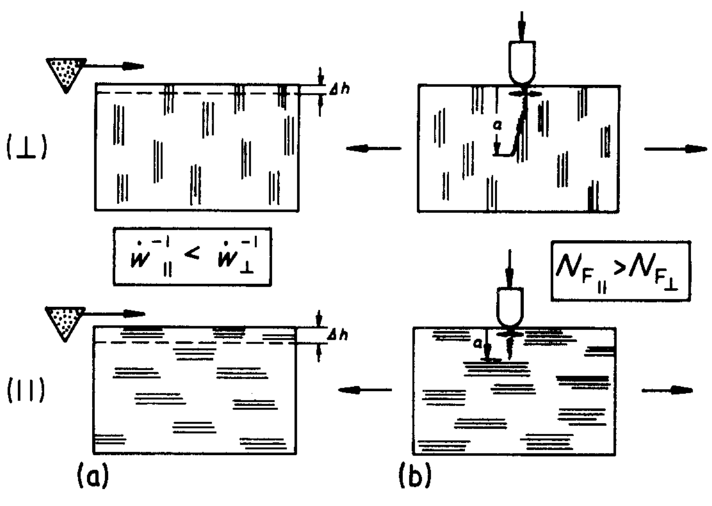

Figure 10 Schematic comparison of the effect of fibre orientation on material's wear resistance (a) and on its fretting fatigue life (b).

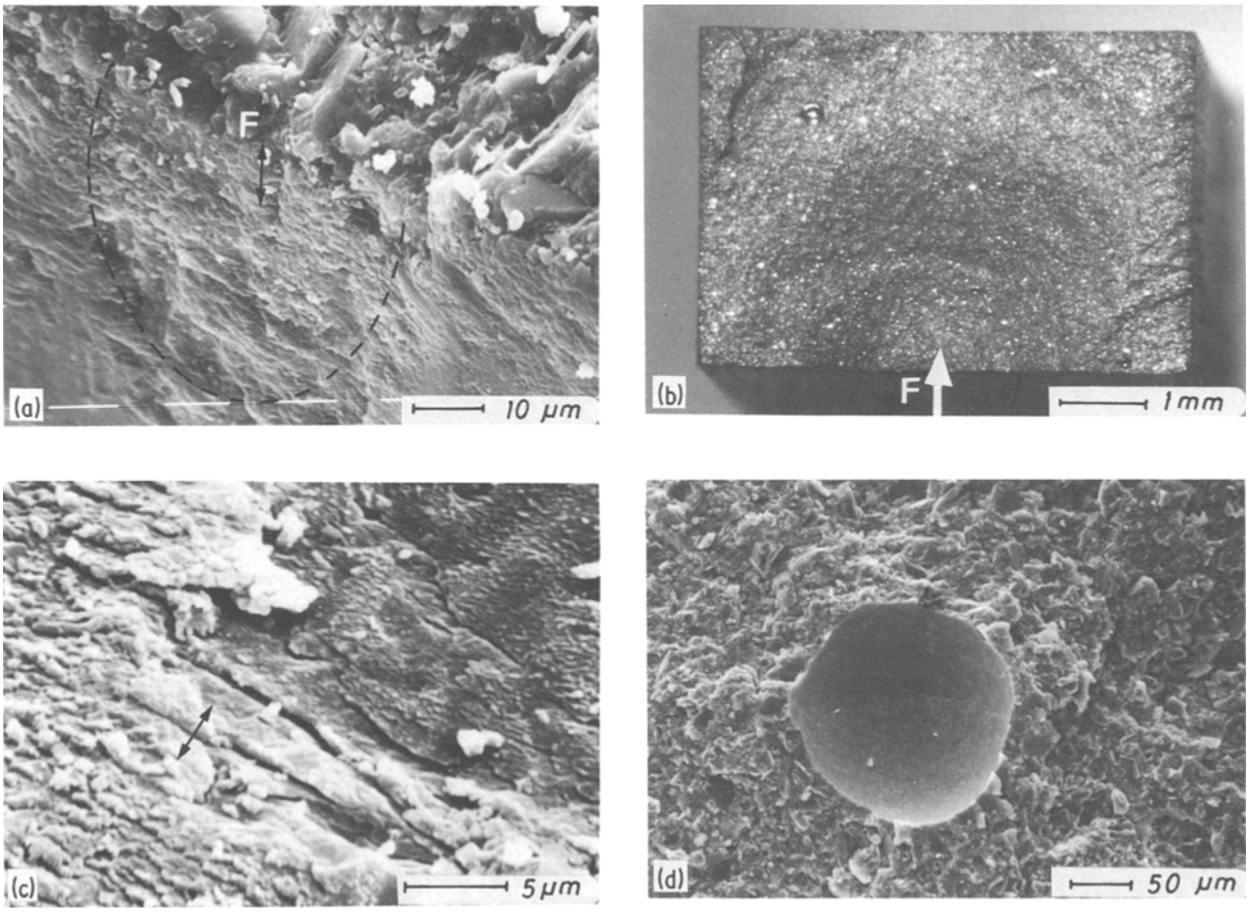

Figure 11 Scanning electron micrographs of fretting fatigued specimens of the UP-matrix material: (a) broken UP-sample with fracture initiated in the fretted region F (dashed line); (b) fracture surface of sample (a), showing fatigue failure initiation at fretting position F; (c) numerous cracks in the fretted region, perpendicular to the slip direction (arrow); (d) void in the matrix as an additional site for fatigue crack initiation.

lowered by simultaneous fatigue and a local, cyclic wear component at the surface (fretting). This is very pronounced for the resin material, whereas the effect of fretting in the case of the composites is a clear function of the fibre orientation in the vicinity of the fretting location.

Acknowledgements
The basic data for the fretting fatigue curves and the fracture and wear properties were generated by Dipl. -Ing. G. Horstenkamp and Dipl. -Ing. E. Reese. Their help in this respect is gratefully acknowledged.

References
1. D. J. GAUL and D. J. DUQUETTE, *Met. Trans.* **11A** (1980) 1581.
2. *Idem, ibid.* **11A** (1980) 1555.
3. S. M. KUDVA and D. J. DUQUETTE, ASTM STP 776 (American Society for Testing and Materials, Philadelphia, Pennsylvania, 1982) pp. 195–203.
4. T. C. CHIEVERS and S. C. GORDELIER, *Wear* **96** (1984) 153.
5. P. J. E. FORSYTH, in "Fretting Fatigue", edited by R. B. Waterhouse (Applied Science, London, 1981) pp. 99–125.
6. K. FRIEDRICH, "Friction and Wear of Polymer Composites, Fortschr. -Ber. VDI-Z., Reihe 18, No. 15 (Verein Deutscher Ingenieure, Düsseldorf, 1984, in English).

Received 5 June
and accepted 10 July 1985